SOCIOECONOMIC ANALYTICS

Using Convolutional Neural Networks for segmentation of brain tumors

Kauã Gabriel Silva de Lima [1] *
Vagner Alves Ferreira da Silva [2]
João Victor Oliveira da Silva [3]
Lucas Patrick Ramos de Oliveira [4]
Diogo Lopes da Silva [5]

[1 2 3 4 5] Pernambuco Federal Institute of Education, Science, and Technology, Palmares, Brazil
Emails: [1] kgsl@discente.edu.br; [2] vafs@discente.ifpe.edu.br; [3] jvos2@discente.ifpe.edu.br;
[4] lpro@discente.ifpe.edu.br; [5] diogo.lopes@palmares.ifpe.edu.br
*Corresponding Author

How to cite this paper: de Lima, K. G. S., da Silva, V. A. F, da Silva, J. V. O., G., de Oliveira, L. P. R., da Silva, D. L. (2024). Using Convolutional Neural Networks for segmentation of brain tumors. *Socioeconomic Analytics,* 2(1), 114-120. https://doi.org/10.51359/2965-4661.2024.265072

RESEARCH ARTICLE

Socioeconomic Analytics
https://periodicos.ufpe.br/revistas/SECAN/
ISSN Online: 2965-4661

Submitted on: 11.11.2024.
Accepted on: 15.12.2024.
Published on: 27.12.2024.

Abstract

This paper presents a brain tumor segmentation system for MRI images using Convolutional Neural Networks (CNNs). The goal is to assist in automated medical analysis by providing accurate segmentations of tumor areas to support diagnosis and treatment planning. The CNN model was trained on MRI images and accurately detected tumor boundaries. The proposed approach utilizes transfer learning to optimize the model's performance on high-resolution images, reducing processing time. The system stands out for its efficiency in segmenting tumors of various sizes and shapes, offering a promising tool for clinical neuroscience.

Keywords

Machine Learning, Neural Networks, healthcare, tumors

1. Introduction

Segmentation of brain tumors in magnetic resonance imaging (MRI) is a crucial step in diagnosis and therapeutic planning, playing a crucial role in detecting tumor areas. However, this challenge is accentuated by the vast variation in the shape, size, and location of tumors, as well as the complexity of the images produced. Usually, this evaluation requires the participation of specialists, being a laborious and error-prone procedure.

Advances in artificial intelligence, particularly deep learning, have transformed the segmentation of medical images. Models such as YOLOv11 (You Only Look Once, version 11) are notable for their ability to identify objects accurately and quickly, even in complex situations. This study describes a brain tumor segmentation method that uses YOLO, improved through transfer learning methods to handle high-definition images effectively.

The central purpose of this research is to create an accurate and fast instrument that helps health professionals detect brain tumors, improving diagnosis and assisting in treatment planning. The goal of the proposal is to shorten the duration of manual analysis, improve the consistency of results, and possibly improve clinical outcomes.

2. Material and Methods

For the development of the brain tumor segmentation model, we used the Ultralytics framework, built on PyTorch. This library was chosen for its flexibility and adaptability to pre-trained models, such as YOLO (Redmon, 2015), ResNet (He, 2016), DDRNet (Hong, 2021), among others. Ultralytics allows for simplified hyperparameter configurations and offers broad compatibility with other libraries, facilitating integration and making the configuration process more straightforward and efficient. The application of methods such as transfer learning is frequent in detection and segmentation models, as highlighted by (da Silva, 2017) in his research on trait optimization and model choice. Its effectiveness in accelerating training and improving performance is widely recognized.

We chose the YOLOv11 model due to its high performance in object detection and its processing speed, fundamental characteristics to achieve accurate and efficient segmentation. In addition, models such as U-Net, widely used in medical image segmentation (Ronneberger, Fischer, & Brox, 2015), have also demonstrated great effectiveness in similar tasks, although YOLOv11 stood out for its speed and real-time accuracy. Figure 1 presents an image of the architecture of YOLO, highlighting its structure and key components. The system was trained in a local environment, using a Ryzen 7 5700U processor with 32GB of RAM, which ensured the ability to handle large volumes of data and process high-resolution images.

To optimize performance, we employ a pre-trained model, applying transfer learning to speed up the process and reduce image processing time. This approach is widely used in detection networks, as discussed by (Silva and Candido, 2016) in their methodology for knowledge extraction in computer networks, which emphasizes the importance of integrating advanced technologies to optimize the use of neural networks in complex contexts such as medical diagnosis.

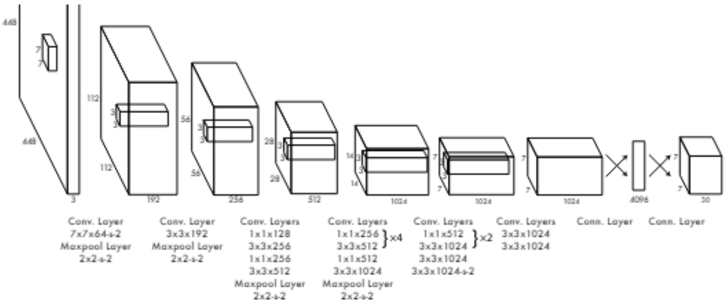

Figure 1. Detection network architecture with 24 convolutional layers and 2 connected.

The dataset (Brain MRI Tumor Segmentation Dataset open Source Dataset, 2024), consisting of 1,937 images, was divided into three subsets: 70% for training, 20% for validation, and 10% for testing. This division ensured a robust evaluation of the model, allowing the analysis of its generalization capacity. The yield analysis of this model was done based on common metrics in the field of object detection, providing a complete perspective of its predictive capacity and the overall quality of the predictions (da Silva, 2017).

The main performance metrics used include Accuracy in equation (1), which measures the proportion of correct predictions in relation to the total samples analyzed; the Recall in equation (2), which evaluates the proportion of correct detections in relation to the total number of real objects present; Precision in equation (3), which measures the proportion of correct detections in relation to the total number of detections performed; and the F1-score in equation (4), which represents the harmonic mean between Accuracy and Recall. Together, these metrics provide a comprehensive assessment of the model's performance, balancing the ability to correctly detect objects, the quality of detections performed, and the overall percentage of hits.

$$Accuracy \ \frac{TP+TN}{TP+TN+FP+FN} \tag{1}$$

- TP: True Positive.
    - Tumors correctly detected by the model. Represents cases where the model marked an area as a tumor and this prediction was correct.
- TN: True Negative.
    - Areas correctly identified as non-tumor. It represents the cases in which the model indicated the absence of a tumor in an area, and this was correct.
- FP: False Positive.
    - Incorrect tumor detections. Represents the cases where the model marked an area as a tumor, but there was actually no tumor.
- FN: False Negative.
    - Tumors not detected by the model. Represents cases in which the model could not identify the presence of a tumor that actually existed.

$$Recall = \frac{TP}{TP+FN} \tag{2}$$

- TP: True Positive.

  - Same concept used in *Accuracy*.

- FN: False Negative.
  - Same concept used in *Accuracy*.

$$Precision = \frac{TP}{TP+FP} \tag{3}$$

- TP: True Positive.
  - Same concept used in *Accuracy*.

- FP: False Positive.
  - Same concept used in *Accuracy*.

$$F1 = 2.\frac{Precision.Recall}{Precision + Recall} \tag{4}$$

3. Results and Discussion

The total training time was 24 hours, using the settings detailed in the Materials and Methods section. The model was trained for 100 epochs, and the 35th epoch presented the best results, as highlighted in Table 1. These results demonstrate the efficacy and potential of the brain tumor segmentation system, evidencing its ability to generate accurate and high-quality segmentations.

The detailed evaluation of the model is presented by Figure 2, which shows the confusion matrix generated during the tests. The model correctly identified 121 tumors (True Positives - TP), with only 2 cases of tumors not detected (False Negatives - FN). In addition, no False Positives (FP) were recorded, while 70 regions were correctly classified as healthy areas (True Negatives - TN).

The accuracy, recall, and F1 score values presented in Table 1 reinforce the high performance of the model:

Table 1. Model performance metrics for brain tumor segmentation, including accuracy, recall, and F1 Score for masks and bounding boxes.

Metrics	Description	Value
Accuracy	Measures the ratio of correct predictions to total samples.	98%
Precision	Accuracy of predictions in the segmentation mask.	98%
Recall	Ability to correctly identify segmentations.	100%
F1 Score	Harmonic average between precision and *recall*.	99%

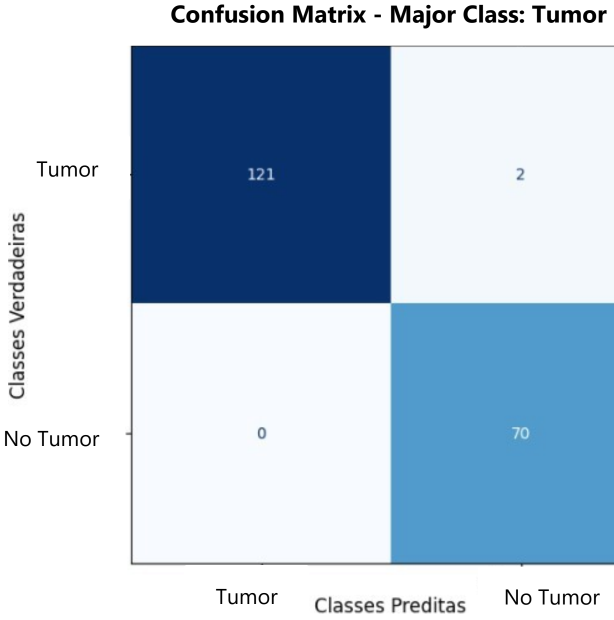

Figure 2. Confusion matrix generated during brain tumor segmentation model evaluation.

These results highlight the robustness of the model, with high performance in the main metrics evaluated. The combination of high accuracy and recall indicates that the system is able to reliably identify and target tumor areas on MRI images. To illustrate the effectiveness of the model, Figures 3, 4 and 5 present two brain magnetic resonance images: The original and the one processed by the system, highlighting the segmentation of the tumor region. This visualization reinforces the model's potential for practical application in medical diagnostics, contributing to clinical aid and decision-making.

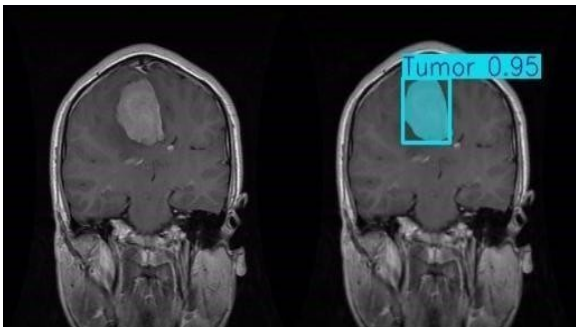

Figure 3. Tumor Detection and Segmentation with Bounding Box.

Figure 3 shows the detection of the brain tumor performed by the system, with the bounding box highlighting the area identified as tumor. On the left, the original magnetic resonance imaging is presented, while on the right, the image processed by the system displays the bounding box over the tumor region, with the segmentation of the tumor area visible at the back of the skull. Segmentation is performed precisely, clearly separating the tumor region from the healthy part of the brain tissue. This visualization highlights the effectiveness of the model in identifying and highlighting tumor areas on the image.

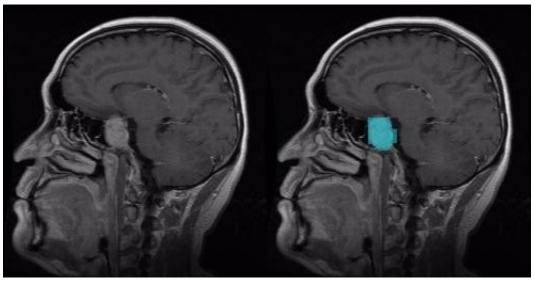

Figure 4. Segmentation without Bounding Box - Lateral View of the Skull.

In Figure 4, the bounding box has been removed, showing only the segmentation of the brain tumor. On the left, the original image and, on the right, the image processed by the system, highlighting the lateral region of the skull and offering a clearer visualization of the tumor segmentation, without distractions.

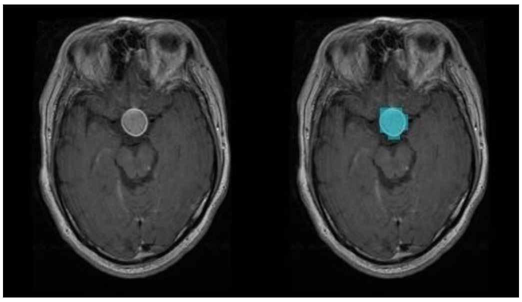

Figure 5. Segmentation without Bounding Box - Top View of the Skull.

Figure 5 also shows the segmentation of the brain tumor, but now visualized from the superior perspective of the skull. As in the previous figures, on the left we see the original and, on the right, the processed image, with the tumor segmentation clearly highlighted in the brain region. Removing the bounding box and changing perspective provides a detailed and accurate view of the location and extent of the tumor in the upper part of the skull. This visualization offers a more detailed assessment of segmentation across different anatomical perspectives of the brain.

4. Conclusion

The identification of brain tumors on magnetic resonance imaging using convolutional neural networks (CNNs) has been shown to be a highly effective strategy to support diagnosis and treatment planning. The developed model, based on the YOLOv11 architecture and optimized by transfer learning, obtained excellent results in the metrics of Accuracy, Precision, Recall, and F1-Score, both for the segmentation of the masks and for the identification of tumor regions. The experimental results indicate that the system is able to identify and segment tumor regions with high precision, positioning itself as a promising tool for the automated analysis of medical images. The high performance of the model, together with the significant reduction in processing time, makes this approach advantageous for clinical use, allowing faster and more accurate diagnoses of brain tumors. However, to further optimize the results, future studies may explore expanding the dataset and fine-tuning the model parameters to improve generalization to different tumor types. Such advances can further strengthen the application of this technology in clinical scenarios, offering a robust and reliable tool for healthcare professionals.

References

1. Brain MRI Tumor Segmentation Dataset. (2024). *Brain MRI Tumor Segmentation* [Dataset]. Roboflow Universe. https://universe.roboflow.com/brain-mri-tumor-segmentation/brain-mri-tumor-segmentation-1d0nw. Visitado em 11-10-2024.
2. da Silva, D. L., Seijas, L. M., & Bastos-Filho, C. J. (2017). Otimização por colônia artificial de abelhas para seleção de características no reconhecimento de sinais de trânsito. International Journal of Swarm Intelligence Research (IJSIR), 8(2), 50–66.ion for feature selection of traffic sign recognition. Int J Swarm Intell Res (IJSIR) 8(2):50–66
3. He, K., Zhang, X., Ren, S., & Sun, J. (2016). Deep residual learning for image recognition. *Proceedings of the IEEE Conference on Computer Vision and Pattern Recognition*, 770-778.
4. Hong, Y., Gao, L., Chen, J., & Shi, M. (2021). Deep dual-resolution networks for real-time and accurate semantic segmentation of road scenes. *arXiv preprint arXiv:2101.06085*.
5. Redmon, J., Divvala, S., Girshick, R., & Farhadi, A. (2015). You Only Look Once: Unified, real-time object detection. *University of Washington, Allen Institute for AI, Facebook AI Research*.
6. Silva, D. L., & Candido, E. A. (2016). Metodologia para extração de conhecimento em redes de computadores. *XI Congresso Norte Nordeste de Pesquisa e Inovação*, Maceió, AL, Brasil.
7. Ronneberger, O., Fischer, P., & Brox, T. (2015). U-Net: Convolutional networks for biomedical image segmentation. *In International Conference on Medical Image Computing and Computer-Assisted Intervention* (pp. 234-241). Springer, Cham. https://doi.org/10.1007/978-3-319-24574-4_28